

# Energy Dependence of the Delta Resonance: Chiral Dynamics in Action

A. M. Bernstein<sup>1</sup> and S. Stave<sup>2</sup>

<sup>1</sup> Physics Department and Laboratory for Nuclear Science, MIT, Cambridge, MA 02139, USA

<sup>2</sup> Department of Physics, Duke University, Durham, North Carolina 27708, USA and Triangle Universities Nuclear Laboratory, Durham, North Carolina 27708, USA

**Abstract.** There is an important connection between the low energy theorems of QCD and the energy dependence of the  $\Delta$  resonance in  $\pi$ -N scattering, as well as the closely related  $\gamma^*N \rightarrow N\pi$  reaction. The resonance shape is due not only to the strong  $\pi$ -N interaction in the p wave but the small interaction in the s wave; the latter is due to spontaneous chiral symmetry breaking in QCD (i.e. the Nambu-Goldstone nature of the pion). A brief overview of experimental tests of chiral perturbation theory and chiral based models is presented.

## 1 Introduction

Since the discovery of the  $\Delta$  resonance<sup>1</sup> (the first excited state of the nucleon) by Fermi's group[2] it has been well known that it dominates low energy  $\pi$ N scattering and the closely related  $\gamma^*N \rightarrow \pi N$  reaction. In the intervening years there has been a great deal of experimental and theoretical activity in this classical field of  $\pi N$  physics. This is central to our understanding of nuclei (the nucleon-nucleon potential) and of the long range properties of hadrons through their virtual emission and absorption of pions. In this article we shall stress the less well known relationship between the spontaneous hiding of chiral symmetry in QCD, its subsequent low energy theorems, and the energy dependence of the  $\Delta$  resonance. A brief overview of low energy  $\pi$ N physics is presented with an emphasis on electromagnetic pion production. It is shown that theoretical calculations based on spontaneous chiral symmetry hiding economically summarize the wealth of accurate data that have been taken in the past two decades[3, 4, 5]. We present this as a tribute to S. N. Yang who has been a leader in using a chiral

---

<sup>1</sup>The modern values for the  $\Delta$  are  $I(J^P)=3/2(3/2^+)$ , center of mass energy  $W = 1232$  MeV, width  $\Gamma = 118$  MeV[1].

based pion cloud model (the Dubna-Mainz-Taipei or DMT model[6]) to successfully predict the observables in these low energy reactions.

The QCD Lagrangian can be written as a sum of two terms,  $L_0$  which is independent of the lightest quark masses (up, down) and  $L_m$  which contains the masses of the two light quarks[7]. Consider the chiral limit in which the light quark masses  $m_q \rightarrow 0$ . As is well known, the vector current is conserved while the axial vector current is conserved only in the chiral limit (i.e.  $m_q \rightarrow 0$ ) and slightly non-conserved in the real world. This is one of the approximate symmetries of QCD on which chiral perturbation theory (ChPT) is based[3, 4, 7]. Despite the fact that the light quark mass independent part of the QCD Lagrangian,  $L_0$ , has chiral symmetry, matter does not seem to obey the rules. The chiral symmetry is expected to show up by the parity doubling of all hadronic states: i.e., the proton with  $j^p = 1/2^+$  would have a  $1/2^-$  partner (the Wigner-Weyl manifestation of the symmetry). Clearly, this is not the case. This indicates that the symmetry is spontaneously hidden (often stated as spontaneously broken) and is manifested in the Nambu-Goldstone mode; the parity doubling occurs through the appearance of a massless pseudo scalar ( $0^-$ ) meson. The opposite parity partner of the proton is a proton and a “massless pion” (Goldstone Boson). The consequence of this for the  $\pi N$  interaction in momentum space is:

$$V_{\pi N} = g_{\pi N} \boldsymbol{\sigma} \cdot \mathbf{p}_\pi \quad (1)$$

where  $\boldsymbol{\sigma}$  is the nucleon spin and  $\mathbf{p}_\pi$  is the pion momentum. In accordance with Goldstone’s theorem, this interaction  $\rightarrow 0$  as the pion momentum  $\rightarrow 0$ . Furthermore, the coupling constant  $g_{\pi N}$  can be computed from the Goldberger-Treiman relation[7] and chiral corrections[8] and is accurate to the few % level. The  $\pi N$  interaction is very weak in the s wave and strong in the p wave which leads to the  $\Delta$  resonance, the tensor force between nucleons, and to long range non-spherical virtual pionic contributions to hadronic structure. These salient features of the  $\pi N$  interaction have been known for decades and can be found in most textbooks on nuclear physics. However, they are usually based on empirical findings such as the pseudoscalar nature of the pion and on the empirically determined coupling constant  $g_{\pi N}$ . What is different in this presentation is the fact that it is based on QCD and that these empirical findings are in fact predicted by the considerations of spontaneous chiral symmetry hiding in QCD.

Equation (1) shows that the cross sections for  $\pi N$  scattering must go to zero at low energies in the chiral limit. This was first derived before the advent of QCD using current algebra (now recognized as the lowest order chiral perturbation theory (ChPT) calculation  $O(p^2)$ ) for  $a(\pi, h)$ , the s wave  $\pi$  hadron scattering length[9]. The result is  $a^I(\pi, h) = -\mathbf{I}_\pi \cdot \mathbf{I}_h m_\pi / (\Lambda_x F_\pi)$  where  $\mathbf{I} = \mathbf{I}_\pi + \mathbf{I}_h$  is the total isospin,  $\mathbf{I}_\pi$  and  $\mathbf{I}_h$  are the isospin of the pion and hadron respectively,  $F_\pi$  is the pion decay constant, and  $\Lambda_x = 4\pi F_\pi \simeq 1$  GeV is the chiral symmetry breaking scale[9]. Note that  $a(\pi, h) \rightarrow 0$  in the chiral limit,  $m_\pi \rightarrow 0$ , as it must to obey Goldstone’s theorem. Also note that  $a(\pi, h) \simeq 1/\Lambda_x \simeq 0.1$  fm, which is small compared to a typical strong interaction scattering length of  $\simeq 1$  fm. This small scattering length is obtained from the explicit chiral symmetry breaking due to the finite quark masses. The predictions of ChPT for  $\pi N$  scattering lengths have

been verified in detail in a beautiful series of experiments on pionic hydrogen and deuterium at PSI[10].

Low energy electromagnetic production of Goldstone Bosons is as fundamental as Goldstone Boson scattering for two reasons: 1) the production amplitudes vanish in the chiral limit (as in scattering); and 2) the phase of the production amplitude is linked to scattering in the final state by unitarity or the final state interaction (Fermi-Watson) theorem suitably modified to take the up, down quark masses into account[11]. First consider the low energy limit of the electric dipole  $E_{0+}$  for s wave photo-pion production[12]:

$$\begin{aligned} E_{0+}(\gamma p \rightarrow \pi^0 p) &= -D_0 \mu (1 + O(\mu) + \dots) \rightarrow 0 \\ E_{0+}(\gamma p \rightarrow \pi^+ n) &= \sqrt{2} D_0 / (1 + \mu + \dots)^{3/2} \rightarrow \sqrt{2} D_0 \\ \mu &= m_\pi / M \rightarrow 0 \\ D_0 = e \cdot g_{\pi N} / 8\pi M &= 24 \cdot 10^{-3} (1/m_\pi) \end{aligned} \quad (2)$$

where  $M$  is the nucleon mass and the right arrow denotes the chiral limit ( $m_u, m_d, m_\pi \rightarrow 0$ ). Equation (2) shows that for neutral pion production the amplitude vanishes in the chiral limit. For charged pion production, there is a different low energy theorem[12]. Therefore, the amplitude that is most sensitive to explicit chiral symmetry breaking is neutral pion production and most of the modern experiments have concentrated on this channel. In general, ChPT to one loop calculated in the heavy Fermion approximation has been highly successful in calculating the observed cross sections and linearly polarized photon asymmetry[12].

## 2 $\pi N$ and $\gamma N \rightarrow \pi N$ Experiments

### 2.1 Energy Dependence of the $\Delta$ Resonance

The application of the ideas of the previous section to data from low energy  $\pi N$  scattering and electromagnetic pion production from the nucleon is instructive. In this section we shall take a broad view of the energy dependence of the  $\pi N$  interaction from threshold through the  $\Delta$  resonance as revealed by total cross section data (amplifying a brief previous presentation[5]). Figure 1 shows the total cross sections for  $\pi^{+/-} p$  scattering[13]. These reactions have a strong  $\Delta$  resonance. As expected, the  $\pi^+ p$  cross section goes to zero near threshold. The small, but not zero, cross section for  $\pi^- p$  scattering near threshold is due to Coulomb effects. These two cross sections clearly show the  $\Delta$  resonance without any interference (the small shift between them is due to the mass difference of the  $\Delta^0$  and  $\Delta^+$ ). Indeed these cross sections are a textbook example of an isolated resonance. Although not usually mentioned in textbooks it is the combination of a strong resonance and a small cross section at threshold that produces this beautiful example (as predicted by chiral dynamics)! This can be verified experimentally in the case of photo-pion production shown in Fig. 2. If we consider the  $\gamma p \rightarrow \pi^0 p$  reaction, the cross section near threshold goes to zero as indicated by Eq. (2) and the  $\Delta$  resonance looks very similar to  $\pi N$  scattering. On the other hand, for the  $\gamma p \rightarrow \pi^+ n$  reaction there is strong s wave production starting at threshold, due to the Kroll-Ruderman low energy theorem (see Eq. (2)). In this

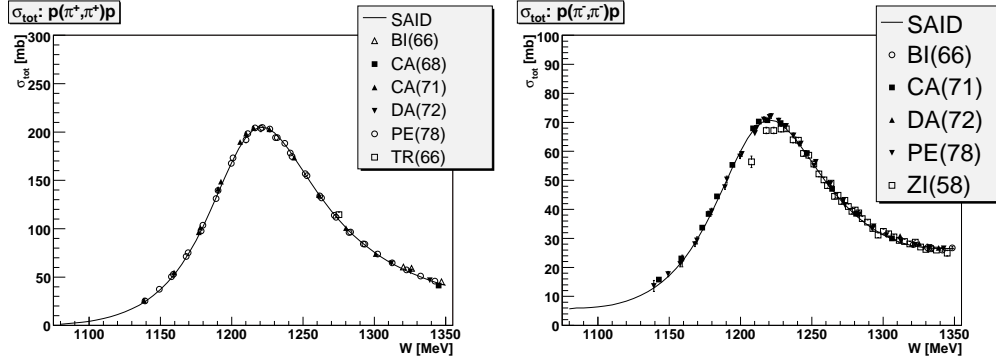


**Figure 1.** The total cross section for  $\pi N$  scattering at low energies as a function of  $W$ , the center of mass energy, through the  $\Delta$  resonance. Left panel:  $\pi^+ p$  scattering. Right panel:  $\pi^- p$  scattering. The data and the fits are from the SAID compilation[13].

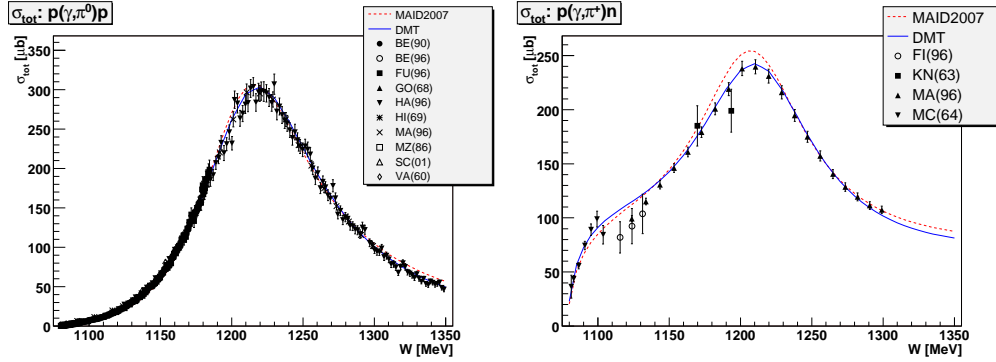


**Figure 2.** The  $\gamma p \rightarrow \pi N$  cross sections as a function of  $W$ , the center of mass energy, from threshold through the  $\Delta$  region. Left panel:  $\gamma p \rightarrow \pi^0 p$ . Right panel:  $\gamma p \rightarrow \pi^+ n$ . The data are from the SAID compilation[13] and the curves represent the results of the DMT[6] and MAID models[14].

case the  $\Delta$  resonance curve is superimposed on the strong s wave amplitude and looks quite different!

From Figure 2 we see that the two model curves are in good agreement with the data. These are the phenomenological MAID[14] and the pion cloud DMT (Dubna-Mainz-Taipei)[6] models, in which S. N. Yang plays a major role. The reason for this good agreement with experiment is that both models have the low energy theorems of QCD as well as an accurate description of the  $\Delta$  resonance.

The energy dependence of the  $\Delta$  resonance can also be seen very clearly in the  $\delta_{33}$  ( $I = J = 3/2$ ) phase shift in  $\pi N$  scattering and in the  $M_{1+}$  ( $I = 3/2$ ) for the  $\gamma^* N \rightarrow \pi N$  reaction (for the notation see [15, 16]). These have the advantage that they show the resonance directly. Since the observables are bilinear combinations of the transition matrix elements neither the phase shifts nor multipoles are directly observable. In general they have been extracted from experiment by

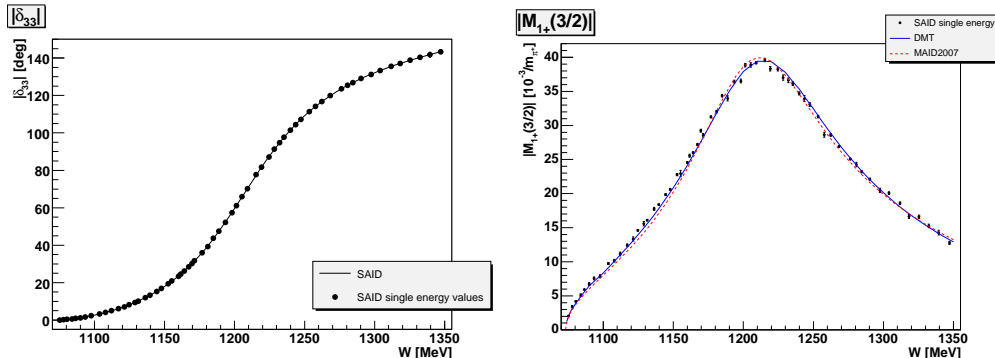


**Figure 3.** Left panel: The  $\delta_{33}$  phase shift for  $\pi N$  scattering versus  $W$ , the center of mass energy, from threshold through the  $\Delta$  resonance. The points are the SAID single energy fits to the data and the curve is the smooth energy dependent fit[13]. Right panel: The absolute value of the resonant  $M_{1+}(I = 3/2)$  multipole for the  $\gamma p \rightarrow \pi N$  reaction as a function of  $W$ . The points are from the SAID single energy analysis[13] and the curves are the results of the DMT[6] and MAID[14] models.

model dependent methods. In this case, where we are exhibiting the dominant amplitudes, the model errors are believed to be small. In Figure 3 we present these quantities from the SAID analysis[13]. It can be seen that  $\delta_{33}$  for  $\pi N$  scattering passes through  $90^\circ$  in the upwards direction at  $W = 1232$  MeV which defines the  $\Delta$  resonance position. The width comes from a Breit-Wigner fit to the energy dependence. The magnitude of the resonant  $M_{1+}(I = 3/2)$  amplitude for the  $\gamma N \rightarrow \pi N$  reaction is also shown in Fig. 3. It also defines the same position and width for the  $\Delta$  as does  $\pi N$  scattering. It can also be seen that the MAID[14] and SAID[13] models are in good agreement with this dominant photo-pion resonant amplitude.

## 2.2 Tests of Theoretical Calculations

In this section we give a brief overview of the present status of experimental tests of chiral perturbation theory (ChPT) and pion cloud model calculations of the electromagnetic pion production for the threshold and  $\Delta$  regions.

A great deal of effort has gone into the study of the near threshold  $\gamma p \rightarrow \pi^0 p$  reaction experimentally at Mainz[17] and Saskatoon[18] and with ChPT calculations[12]. The unpolarized cross sections were accurately measured and, despite their small size, the results from Mainz and Saskatoon are in reasonable agreement. The experiments were performed using tagged photons for energies between threshold (144.7 MeV) and 166 MeV. For the Mainz data there were sufficient statistics to bin the cross section data in  $\simeq 1$  MeV steps. The ChPT calculations[12] have proven to be quite accurate in fitting the cross sections with only five empirical low energy constants at  $O(p^4)^2$ . In addition, the polarized

<sup>2</sup>Due to correlations in the fitting there are effectively only three independent low energy parameters.

linear photon asymmetry  $\Sigma$  was also measured at Mainz. Here the statistics only allowed us to group the data from threshold to 166 MeV in one cross section averaged energy bin of 159.5 MeV[17]. The results are shown in Fig. 4. Here the improvement in the  $O(p^4)$  ChPT calculation over the  $O(p^3)$  version is seen. This is obtained by fitting the data using the additional low energy constants that appear at  $O(p^4)$ . This is an indication of how sensitive this observable is to the small p wave multipoles. Another indication of this is that the dispersion theory calculation, which does agree with the unpolarized cross section data, does not agree with  $\Sigma$ . This is probably due to a small discrepancy in the  $M_{1-}$  multipole which is not well constrained by the other data on which this calculation is based. More recent data taken at Mainz are anticipated to produce five values of  $\Sigma$  between threshold and 168 MeV[19].

Most of the dynamical models do not accurately predict cross sections for the near threshold  $\gamma p \rightarrow \pi^0 p$  reaction. The exception to this is the DMT model which has accurately predicted the observed cross sections[20, 6]. However, it does not accurately predict the polarized photon asymmetry  $\Sigma$ . Again, as a sign of the extreme sensitivity of this observable, when they arbitrarily reduce their  $M_{1-}$  amplitude by 15% they have agreement with the observed value of  $\Sigma$  shown in Fig. 4. However the prediction of this amplitude is not as robust due to the tail of the Roper resonance, vector meson effects, and final state interactions[20, 6].

Having discussed the comparison between the calculations and experiment it is of interest to look at the major ingredients of the ChPT[12] and DMT[6, 20] calculations. ChPT employs chiral symmetric Lagrangians with explicit chiral symmetry broken by the quark mass terms. It is an order by order expansion in which unitarity is restored as the order increases. For example, at the tree level unitarity is completely absent, but is mostly restored by the one loop calculations[12]. It is gauge invariant and preserves crossing symmetry. By contrast the DMT model has chiral symmetry in the Lagrangian and is unitary to all orders: it uses a pion cloud model for the  $\pi N$  t matrix which gives good agreement with the  $\pi N$  phase shifts[21]. It enforces gauge invariance but violates crossing symmetry.

A sensitive way to compare theory and experiment is at the level of the multipoles. Since the observables are bilinear combinations of the multipoles[16] this process is often model dependent. However, in the case of near threshold pion production an approximate, but reasonably accurate, model independent multipole extraction is possible. This is because there are only five real numbers to extract from the experiments (see e.g. [22] for a more detailed discussion). These are the s wave electric dipole amplitude  $E_{0+}$  which is complex, and three p wave amplitudes which are approximately real numbers in this energy region. Due to the low energy theorems of QCD[12] (see Eq. (2)) the p wave amplitudes tend to dominate even relatively close to threshold. The real part of the s wave electric dipole amplitude  $\text{Re}E_{0+}$  is extracted from the data using the interference between s and p waves which goes as  $\cos(\theta_\pi)$  in the differential cross section and leads to significant errors. The results for  $\text{Re}E_{0+}$  versus photon energy are plotted in Fig. 4. There is reasonable agreement between the Mainz and Saskatoon points as well as with ChPT[12] and the unitary model calculations[22]. The sharp downturn in  $\text{Re}E_{0+}$  between the threshold at 144.7 MeV and the  $\pi^+ n$

threshold at 151.4 MeV is due to a unitary cusp caused by the interference between the  $\gamma p \rightarrow \pi^0 p$  and  $\gamma p \rightarrow \pi^+ n$  channels[11]. The magnitude of the cusp is  $\beta = \text{Re}E_{0+}(\gamma p \rightarrow \pi^+ n) \cdot a_{cex}(\pi^+ n \rightarrow \pi^0 p)$  which is measured to an accuracy of  $\simeq 30\%$  from the data shown[22]. The reason for this accuracy limitation is due to the fact that in addition to the experimental errors in  $\text{Re}E_{0+}$ , this quantity is a sum of a (not precisely known) smooth function and a more rapidly varying cusp[11, 22]. Therefore it is important to measure  $\text{Im}E_{0+}$  which starts from close to zero at the  $\pi^+ n$  threshold energy and rises rapidly as  $\beta p_{\pi^+}$ . This makes the extraction of  $\beta$  as accurate as the measured asymmetry for  $\pi^0$  photoproduction from a polarized target normal to the reaction plane. We are planning to conduct future experiments at HI $\gamma$ S, a new photon source being constructed at Duke[23]. These experiments will have full photon and target polarization and will be a significant extension of the results we have at present. The estimated error for such an experiment running at HI $\gamma$ S for  $\simeq 200$  hours of anticipated operation of the accelerator per data point is presented in Fig. 4 for  $\text{Re}E_{0+}$ . There are equally small error bars estimated for the asymmetry measurement for unpolarized photons and a transversely polarized proton target. This experiment will allow us to extract  $\text{Im}E_{0+}$ . Combining this with an independent measurement of the  $\gamma p \rightarrow \pi^+ n$  cross section will allow us to extract  $\beta$  at the few % level and measure the charge exchange scattering length  $a_{cex}(\pi^+ n \rightarrow \pi^0 p)$  for the first time. We will be able to compare this to the measured value of  $a_{cex}(\pi^- p \rightarrow \pi^0 n)$ [10] as an isospin conservation test. This illustrates the power of photo-pion reaction studies with transversely polarized targets to measure  $\pi N$  phase shifts in completely neutral charge channels which are not accessible to pion beam experiments! This is potentially valuable to help pin down experimentally the value of the  $\pi N - \sigma$  term which has had a long, difficult measurement history.

Although ChPT has been extremely successful in predicting the cross sections and the linearly polarized photon asymmetry in the  $\gamma p \rightarrow \pi^0 p$  reaction there is a significant discrepancy with the  $ep \rightarrow e' p \pi^0$  reaction data at  $Q^2 = 0.05 \text{ GeV}^2/c^2$  taken at Mainz[25] shown in Fig. 5. It can be seen that the ChPT calculations[26] do not agree with the data although the DMT dynamical model does[20, 6]. This discrepancy is a potentially serious problem for ChPT which needs to be resolved. The reason is that the present calculations are  $O(p^3)$  and it has been shown that to obtain agreement with the photo-pion data  $O(p^4)$  calculations are needed.

The photo- and electro-pion  $\gamma^* p \rightarrow \Delta$  reactions have been extensively used to study non-spherical amplitudes (shape) in the nucleon and  $\Delta$  structure[27, 28, 29]. This is studied by measuring the electric and Coulomb quadrupole amplitudes (E2,C2) in the predominantly magnetic dipole, quark spin flip (M1)  $\gamma^* N \rightarrow \Delta$  amplitude. At low  $Q^2$  the non-spherical pion cloud is a major contributor to this (for a review see[27, 28, 29]). Figure 6 shows the Bates data[30] for the transverse-longitudinal interference cross section  $\sigma_{LT}$  at  $Q^2 = 0.127 \text{ GeV}^2/c^2$ [30]. This partial cross section is particularly sensitive to the Coulomb quadrupole C2  $\gamma^* N \rightarrow \Delta$  amplitude. This figure shows our best estimate of the difference between the electro-excitation  $\Delta$  for the spherical case (the relatively flat, dark grey band) and the fit to the data which shows the C2 magnitude[31, 32, 33]. The magnitude and  $Q^2$  evolution of the Coulomb

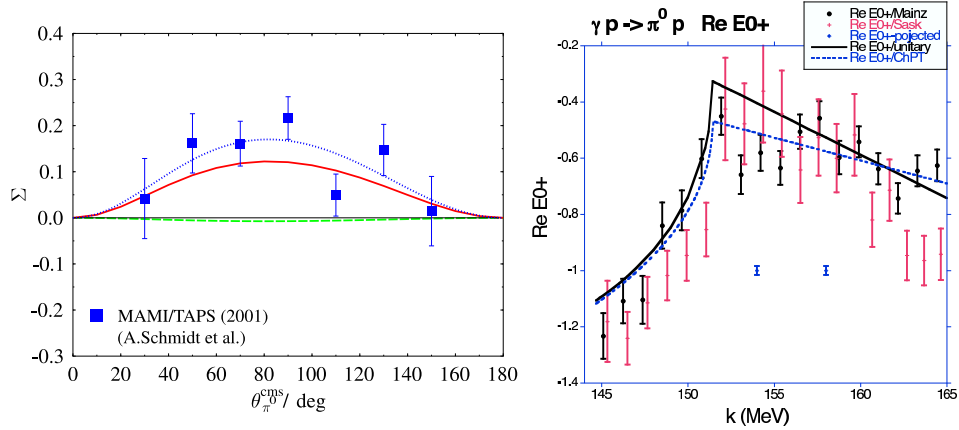


**Figure 4.** The  $\gamma p \rightarrow \pi^0 p$  reaction. Left panel: Polarized photon asymmetry  $\Sigma$  versus angle at an average photon energy of 159.5 MeV[17]. The solid (red) curve is ChPT,  $O(p^3)$ , the dotted (blue) curve is ChPT,  $O(p^4)$ [12]. The dashed (green) curve is from dispersion theory[24]. Right panel:  $\text{Re } E_{0+}$ [15] versus photon energy. The data points are from Mainz[17] and Saskatoon[18]. The curves are from ChPT[12] and a unitary fit to the data[11]. The two projected points from HI $\gamma$ S are plotted at an arbitrary value ( $\text{Re } E_{0+} = -1$ ) to show the anticipated statistical errors for 200 hours of running time per point. See text for discussion.

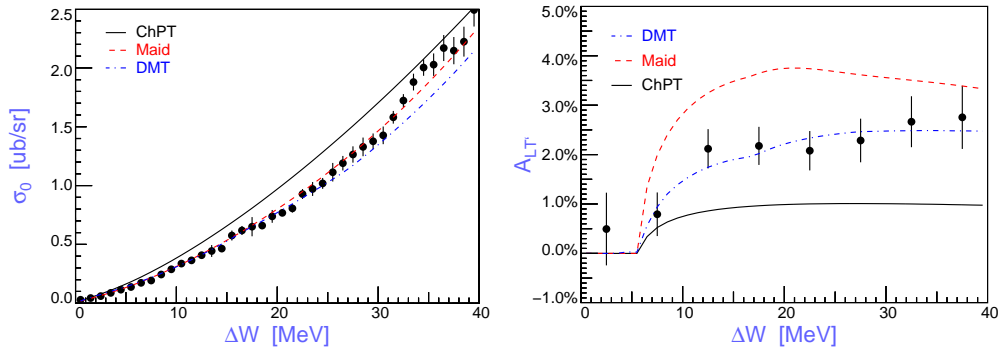


**Figure 5.** Cross section (left panel) and  $LT'$  asymmetry (right panel) for the  $ep \rightarrow e'\pi^0 p$  reaction at  $Q^2 = 0.05 \text{ GeV}^2/c^2$  versus  $\Delta W$ , the center of mass energy above threshold[25]. See text for discussion.



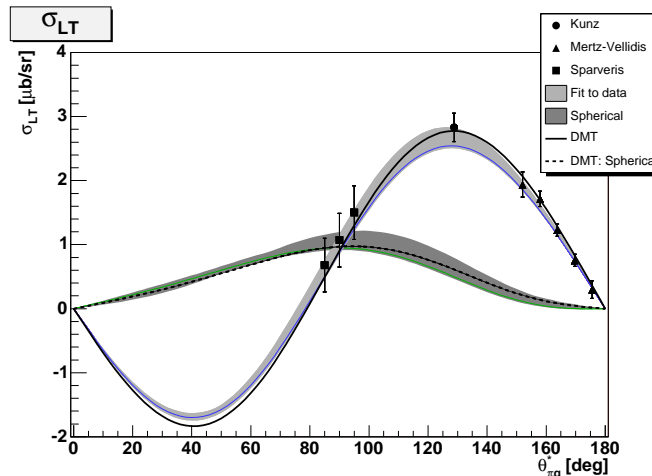


**Figure 6.**  $\sigma_{LT}$  from the  $ep \rightarrow e'\pi^0 p$  reaction at  $Q^2 = 0.127 \text{ GeV}^2/c^2$ ,  $W = 1232 \text{ MeV}$  (see text). The light grey curve is the fit to the data[30] and the relatively flat, dark grey curve shows the calculation for the spherical case, i.e. when the quadrupole transition amplitudes are set to zero[27, 31, 33].

quadrupole amplitude indicates that the quark models do not agree with experiment, but that models with pionic degrees of freedom do[6, 34], demonstrating that the crucial ingredient in the non-spherical amplitude at long range is the pion cloud. More recently there have been chiral-effective field theory calculations of this process[35, 36] which reinforce this observation. As was stated earlier, the presence of long range pionic effects in the non-spherical nucleon and  $\Delta$  amplitudes is expected due to the spontaneous hiding of chiral symmetry and the associated p wave pion-nucleon interaction (see Eq. (1)).

### 3 Conclusions

We have shown that the classical isolated  $\Delta$  resonance energy dependence (which is well known to be a p wave resonance) also depends on the weakness of the s wave amplitude. This behavior is expected on the basis of the spontaneous hiding of chiral symmetry in QCD: it is observed in the total cross sections for  $\pi^{+/-}p$  scattering and in the  $\gamma p \rightarrow \pi^0 p$  reactions. It was shown that in the case of the  $\gamma p \rightarrow \pi^+ n$  reaction, where the Kroll-Ruderman theorem leads to a strong s wave production at threshold, that the energy dependence of the  $\Delta$  resonance appears quite different.

In the well studied, near threshold  $\gamma^* p \rightarrow \pi^0 p$  reaction the agreement between  $O(p^4)$  ChPT calculations and experiment is excellent for the photon data but not so good for electroproduction at  $Q^2 = 0.05 \text{ GeV}^2/c^2$  where the calculations have only been carried out to  $O(p^3)$ , indicating that further work is required. The pion cloud DMT model gives a reasonable description of all of the data. We have also mentioned further experiments which will test the theories

in a more stringent fashion. These include photo-pion production experiments with transversely polarized targets which have the potential to measure  $\pi N$  scattering in previously unexplored charge states ( $\pi^0 n$  elastic scattering and charge exchange). If these can be performed with sufficient accuracy they will subject the theory to stringent tests. In addition, isospin conservation can be checked in a new way.

## References

1. Yao, W.-M. et al.: J. Phys. **G33**, 1 (2006)
2. Anderson, H. L., Fermi, E., Long, E. A., Nagle, D. E.: Phys. Rev. **85**, 936 (1952)
3. Ahmed, M. W., Gao, H., Holstein, B., Weller H. R.(eds.): Workshop on Chiral Dynamics: Theory and Experiment 2006. To be published by World Scientific, editors, <http://www.tunl.duke.edu/events/cd2006/>
4. Bernard, V., Meissner, U.-G.: Submitted to Ann.Rev.Nucl.Part.Sci., [arXiv:hep-ph/0611231 (2006)]; Bernard, V.: [arXiv:hep-ph/0706.0312 (2007)]
5. Bernstein, A. M.: Opening Remarks at Chiral Dynamics 2006: Experimental Tests of Chiral Symmetry Breaking, [arXiv:hep-ph/0707.4250 (2007)]
6. Kamalov, S. S., Yang, S. N.: Phys. Rev. Lett. **83**, 4494 (1999)
7. Donoghue, J. F., Golowich, E. , Holstein, B. R.: Dynamics of the Standard Model. Cambridge ; New York: Cambridge University Press 1992
8. Goity, J. L., Lewis, R., Schvellinger, M., Zhang, L.-Z.: Phys. Lett. **B454**, 115 (1999)
9. Weinberg, S.: Phys. Rev. Lett. **17**, 616 (1966)
10. Gotta, D.: Int. J. Mod. Phys. **A20**, 349 (2005)
11. Bernstein, A. M.: Phys. Lett. **B442**, 20 (1998)
12. Bernard, V. , Kaiser, N., Meissner, U.-G.: Eur. Phys. J. **A11**, 209 (2001); Z. Phys. **C70**, 483 (1996); Phys. Lett. **B383**, 116 (1996)
13. Arndt, R. et al.: Phys. Rev. **C66**, 055213 (2002); <http://gwdac.phys.gwu.edu>
14. Drechsel, D., Hanstein, O., Kamalov, S. S., Tiator, L.: Nucl. Phys. **A645**, 145 (1999); [www.kph.uni-mainz.de/MAID](http://www.kph.uni-mainz.de/MAID)
15. The notation for the  $\gamma^* N \rightarrow \pi N$  amplitudes is: the capital letter  $M, E, L(S)$  stands for the character of the virtual photon, magnetic, electric, or longitudinal (or scalar), the subscript stands for  $l=$  orbital angular momentum of the emitted pion, and the  $\pm$  indicates  $j =$  the total angular momentum of the emitted pion =  $l \pm 1/2$ .

16. Drechsel, D., Tiator, L.: J. Phys. **G18**, 449 (1992); Raskin, A.S., Donnelly, T.W.: Ann. Phys. **191**, 78 (1989)
17. Schmidt, A. et al.: Phys. Rev. Lett. **87**, 232501 (2001)
18. Bergstrom, J. C. et al.: Phys. Rev. **C53**, 1052 (1996)
19. Hornidge, D. : private communication
20. Kamalov, S. S., Chen, G.-Y., Yang, S. N., Drechsel, D., Tiator, L.: Phys. Lett. **B522**, 27 (2001)
21. Hung, C.-T., Yang, S. N., Lee, T.-S. H.: Phys. Rev. **C64**, 034309 (2001)
22. Bernstein, A. M. et al.: Phys. Rev. **C55**, 1509 (1997)
23. <http://higs.tunl.duke.edu>
24. Hanstein, O., Drechsel, D., Tiator, L.: Nucl. Phys. **A632**, 561 (1998)
25. Weis, M. et al.: [arXiv:nucl-ex/0705.3816 (2007)]
26. Bernard, V., Kaiser, N., Meissner, U.-G.: Nucl. Phys. **A607**, 379 (1996); Phys. Rev. Lett. **74**, 3752 (1995)
27. Papanicolas, C., Bernstein, A. M. (eds.): Shape of Hadrons, Athens, Greece, 27-29 April 2006 AIP Conference Proceedings, Volume 904. New York: AIP 2007
28. Bernstein, A. M., Papanicolas, C. N.: AIP Conf. Proc. **904**, 1 (2007)
29. Pascalutsa, V., Vanderhaeghen, M., Yang, S. N.: Phys. Rept. **437**, 125 (2007)
30. Sparveris, N. F. et al.: Phys. Rev. Lett. **94**, 022003 (2005)
31. Papanicolas, C.N.: Eur. Phys. J. **A18**, 141 (2003)
32. Stiliaris, E., Papanicolas, C. N.: AIP Conf. Proc. **904**, 257 (2007)
33. Stave, S., Bernstein, A. M., Nakagawa, I.: AIP Conf. Proc. **904**, 245 (2007)
34. Sato, T., Lee, T.-S. H.: Phys. Rev. **C63**, 055201 (2001)
35. Pascalutsa, V., Vanderhaeghen, M.: Phys. Rev. **D73**, 034003 (2006)
36. Gail, T. A., Hemmert, T. R.: Eur. Phys. J. **A28**, 91 (2006)